Harnessing Genetic Variation in Leaf Angle to Increase Productivity of *Sorghum bicolor*

Sandra K. Truong,*,† Ryan F. McCormick,*,† William L. Rooney,‡ and John E. Mullet*,†,1

*Interdisciplinary Program in Genetics, †Biochemistry and Biophysics Department, and ‡Soil and Crop Sciences Department, Texas A&M University, College Station, Texas 77843

ABSTRACT The efficiency with which a plant intercepts solar radiation is determined primarily by its architecture. Understanding the genetic regulation of plant architecture and how changes in architecture affect performance can be used to improve plant productivity. Leaf inclination angle, the angle at which a leaf emerges with respect to the stem, is a feature of plant architecture that influences how a plant canopy intercepts solar radiation. Here we identify extensive genetic variation for leaf inclination angle in the crop plant *Sorghum bicolor*, a C4 grass species used for the production of grain, forage, and bioenergy. Multiple genetic loci that regulate leaf inclination angle were identified in recombinant inbred line populations of grain and bioenergy sorghum. Alleles of sorghum *dwarf-3*, a gene encoding a P-glycoprotein involved in polar auxin transport, are shown to change leaf inclination angle by up to 34° (0.59 rad). The impact of heritable variation in leaf inclination angle on light interception in sorghum canopies was assessed using functional-structural plant models and field experiments. Smaller leaf inclination angles caused solar radiation to penetrate deeper into the canopy, and the resulting redistribution of light is predicted to increase the biomass yield potential of bioenergy sorghum by at least 3%. These results show that sorghum leaf angle is a heritable trait regulated by multiple loci and that genetic variation in leaf angle can be used to modify plant architecture to improve sorghum crop performance.

S USTAINABLY increasing the productivity of crops on land currently used for agriculture without depleting natural resources is a global priority (Foley *et al.* 2011; Drewry *et al.* 2014). Improving the efficiency with which plants intercept solar radiation is one means to sustainably improve crop productivity. Leaf angle, or leaf erectness, is a plant canopy parameter that has drawn considerable attention because of the predicted improvement in photosynthetic efficiency and reduction in plant stress afforded by the redistribution of solar radiation from upper to lower levels of canopies (Tollenaar and Wu 1999; Duvick 2005; Murchie *et al.* 2009; Zhu *et al.* 2010; Murchie and Reynolds 2012; Drewry *et al.* 2014; Mansfield and Mumm 2014). Performance improvements predicted by theoretical models are corroborated by positive correlations between small leaf angles and cereal crop yields;

post–green revolution rice cultivars have smaller leaf inclination angles and higher yields relative to their pre–green revolution predecessors (Yoshida 1972; Sinclair and Sheehy 1999; Sakamoto *et al.* 2006), and modern maize is also characterized by small inclination angles as a consequence of selection for increased grain yield in breeding programs (Duvick 2005; Lee and Tollenaar 2007; Hammer *et al.* 2009; Tian *et al.* 2011; Mansfield and Mumm 2014).

Despite the association of leaf angle with increased productivity, its genetic basis remains to be fully characterized for many of the major grasses. In maize, *ligueless1* and *ligueless2* have been identified as major regulators of leaf angle that can improve plant productivity (Pendleton *et al.* 1968; Lambert and Johnson 1978; Moreno *et al.* 1997; Walsh *et al.* 1998). More than 40 additional quantitative trait loci (QTL) have been identified in the maize nested association mapping (NAM) and recombinant inbred lines (RIL) populations (McMullen *et al.* 2009; Tian *et al.* 2011; Li *et al.* 2015). In rice, *osdwarf4-1* and *leaf inclination2* have been identified and shown to play roles in plant hormone responses that result in changes in leaf angle (Sakamoto *et al.* 2006; Zhao *et al.* 2010). Progress in identifying leaf angle QTL has been made in sorghum, the fifth most widely produced grain and forage

crop, but a gene that regulates leaf angle has yet to be identified as has been done in maize and rice (Hart *et al.* 2001; Gill *et al.* 2014; Perez *et al.* 2014; Xin *et al.* 2015).

The physiological basis for the impact of leaf inclination angles on yield may be explained by altered vertical distribution of solar radiation in the canopy. Leaf positioning, a factor influenced by leaf inclination angle, can maximize carbon gain by optimizing interception of photosynthetically active radiation (PAR) for canopy photosynthesis and by mitigating heat stress induced by excess infrared radiation (IR) (Zhu *et al.* 2008, 2010; van Zanten *et al.* 2010; Song *et al.* 2013). In addition to mitigating the occurrence of excess radiation at the top of the canopy (Nobel 2005; Long *et al.* 2006; Zhu *et al.* 2010; Mullet *et al.* 2014), canopy architectures that have small upper leaf angles redistribute PAR more uniformly throughout the canopy, thereby reducing shade-induced senescence of lower leaves (Hurng *et al.* 1986; Sinclair and Sheehy 1999; van Zanten *et al.* 2010; Song *et al.* 2013). The resulting increase in green leaf area allows for greater accumulation of nitrogen, a possible rate-limiting factor during grain filling in modern high-yield cultivars (Drouet and Bonhomme 1999; Sinclair and Sheehy 1999; Hammer *et al.* 2009). More optimal vertical redistribution of solar radiation throughout the canopy also allows for denser planting of grain crops, an important factor contributing to increased grain yield per hectare (Sinclair and Sheehy 1999; Duvick 2005; Tian *et al.* 2011; Mansfield and Mumm 2014). For example, small leaf angles of the rice *osdwarf-4* mutant and the maize *liguleless2* mutant enabled higher-density planting that increased biomass yield of the respective crops (Lambert and Johnson 1978; Sakamoto *et al.* 2006).

Given successes in other grass crops, there is strong motivation for identifying the genetic basis of leaf angle and determining its physiological consequences in sorghum, particularly for bioenergy sorghum. High-biomass energy sorghum hybrids have long growing seasons and accumulate most of their biomass in tall ($\sim$4 m) closed canopies (Rooney *et al.* 2007; Olson *et al.* 2012; Mullet *et al.* 2014). Over the long bioenergy growing season, small daily improvements in energy conversion efficiency conferred by more optimal leaf angles could translate into large seasonal increases in biomass accumulation. We examined the genetic basis of leaf inclination angle in sorghum using both grain and bioenergy sorghum RIL populations and identified multiple QTL contributing to the regulation of leaf angle. Moreover, we demonstrate that a leaf angle QTL present in grain sorghum germplasm is caused by sorghum *dwarf-3* (a homolog of maize *br2*) and that the recessive allele of sorghum *dwarf-3* decreases leaf inclination angle up to 34° (0.59 rad). Additionally, we use functional-structural plant modeling and field experiments to show that smaller leaf inclination angles cause solar radiation, including PAR, to penetrate deeper into energy sorghum canopies. The improvement in conversion efficiency afforded by the redistribution of PAR is predicted to increase the biomass yield of bioenergy sorghum over the growing season by at least 3%. Given these results, genetically optimizing leaf angle represents a promising way to sustainably increase sorghum productivity.

Materials and Methods

Genetic basis of leaf inclination angle

Two recombinant inbred line populations generated from biparental crosses of BTx623 × IS3620c ($n = 398$) and R07018 × R07020 ($n = 96$) were used to examine the genetic basis of leaf inclination angle in *Sorghum bicolor* (Burow *et al.* 2011; Bartek *et al.* 2012). Individuals from these populations were genotyped by sequencing using the restriction enzyme–based reduced representation technique Digital Genotyping (Morishige *et al.* 2013). Template DNA was prepared using the restriction enzyme NgoMIV for the BTx623 × IS3620c population and FseI for the R07018 × R07020 population. Libraries were sequenced with an Illumina HiSeq 2500. Reads were mapped to the sorghum reference sequence (Sbi1) with the Burrows-Wheeler Aligner (BWA v0.7.5.a) (Paterson *et al.* 2009; Li and Durbin 2010). Aligned reads were processed with Picard (v1.108), and variant calls (SNPs and indels) were generated using the GATK (v3.2-2) by following the naive pipeline of the RIG workflow (McKenna *et al.* 2010; Depristo *et al.* 2011; Van der Auwera *et al.* 2013; McCormick *et al.* 2015). Subsequent genetic maps were generated using R/qtl (Broman *et al.* 2003). The BTx623 × IS3620C genetic map contained 10,091 markers and was constructed as described in Truong *et al.* (2014) under a model of excess heterozygosity. Genotype data for R07018 × R07020 were quality controlled in a similar manner, and a genetic map containing 1968 markers was estimated as an F_5 using the BC_sF_t Tools in R/qtl. Genetic maps and genotype data are available in the Supporting Information, File S2.

Phenotyping leaf inclination angle

The two experimental crosses used to study the genetic basis of leaf inclination angle, BTx623 × IS3620c and R07018 × R07020, were planted and phenotyped in College Station, Texas, in a greenhouse and in experimental fields. Table 1 provides information on where, when, and the number of individuals from each population that were planted and phenotyped. Phenotypes used in heritability calculations and QTL mapping were the average of the biological replicates measured (Table 1). To phenotype leaf inclination angle, leaves were counted by starting from the youngest ligulated leaf to the older leaves further from the top the plant. That is, at the time of phenotyping, the youngest fully expanded leaf (below the whorl) was identified as leaf 1, and each subsequent leaf was numbered sequentially (*e.g.*, leaf 3 was two leaves below leaf 1). Leaf inclination angle was measured with a protractor; the origin (pinpoint) was placed where the leaf midrib would meet the stem. The angle measured was between the stem and the adaxial midrib of the leaf (the axil).

Stepwise multiple-QTL mapping and heritability estimates

Stepwise multiple-QTL analysis was performed on the genotype and phenotype data described earlier to identify the QTL and epistatic interactions between them that best describe the

Table 1 Experimental crosses and phenotyping metadata

Cross generation	RILs (n)	Location (College Station, TX)	Planting		Phenotyping	
			Date	Structure	Date(s)	Reps.
BTx623 × IS3620c	88	Field	03/27/2013	One-row plot	06/20/2013, 06/26/2013, 06/30/2013	3
F$_{6-8}$	336	Greenhouse	05/27/2014	Two per pot	07/04/2014–07/05/2014	2
	7	Field	04/08/2014	One-row plot	06/18/2014–06/19/2014	4
R07018 × R07020	94	Greenhouse	07/30/2013	Three per pot	09/07/2013	3
F$_5$	94	Field	04/08/2014	One-row plot	06/27/2014	3
	94	Field	04/08/2014	One-row plot	07/31/2014	3
	2	Field	04/08/2014	Four-row plots	07/22/2014–07/26/2014	10

This table contains the two biparental crosses used, the number (n) of RILs assayed, the location, time, and structure of planting, the number of biological replications phenotyped (*i.e.*, number of plants), and the time at which measurements were acquired. Row plots in the field are planted mechanically and are 0.76 m apart and have a planting density of approximately 13.2 plants/m².

genetic basis of variation in leaf inclination angle phenotypes. Phenotype data were normalized by empirical normal quantile transformation (Peng *et al.* 2007). A single QTL analysis using the expectation-maximization (EM) algorithm initially identified primary additive QTL, and this was used to seed model selection for multiple-QTL analysis. We employed the method of Manichaikul *et al.* (2009) for model selection as implemented in R/qtl (Broman *et al.* 2003). This method considers the LOD score for a multiple-QTL model penalized by the complexity of the model, using penalty scores specific to each phenotype. We used computational resources on the Whole Systems Genomics Initiative (WSGI) cluster at Texas A&M University to calculate the penalties for main effects, heavy interactions, and light interactions; these penalties were calculated from 24,000 permutations of each phenotype from each population with genetic markers that were 2 cM apart (∼600 markers) to find a significance level of 5% in the context of a two-dimensional two-QTL genome scan; penalized LOD (pLOD) scores are listed in File S2.

We chose a parsimonious QTL model for each phenotype to report here (detailed statistics of each QTL model are provided in File S2). The models chosen are less prone to false-positive results in our approach to QTL model selection because we required additional QTL and interactions to increase the pLOD of the QTL model by at least its LOD penalties for main and light interactions, respectively. We did not choose an exhaustive QTL model, and less stringent QTL models for the phenotypes are possible.

In addition to variance explained by the QTL, we also estimated the variance explained by SNPs and indels across the genome for each phenotype using GCTA (Yang *et al.* 2011). The genetic variants that were used as input to genetic map construction (prior to the quality control involved in map construction) were quality controlled using PLINK v1.90b3u (Purcell *et al.* 2007), and heritability was estimated using a genomic relationship matrix (GRM) and restricted maximum likelihood (REML) as implemented in GCTA. This analysis estimates the proportion of observed phenotypic variance-covariance relationships among the lines that can be explained by the whole-genome relatedness of the lines estimated by markers, providing an estimate of narrow-sense heritability (Yang *et al.* 2013).

dw3 gene identification

The *dwarf-3* (*dw3*) gene is well known for its effect on stalk height in *S. bicolor*. The common, nonfunctional *dw3* allele contains an 882-bp tandem duplication in exon 5 that causes the loss of function; the null *dw3* allele is genetically unstable and can revert to the functional *Dw3* allele when the 882-bp duplication is removed by unequal crossing over (Multani *et al.* 2003). The reversion event is visually identifiable when it occurs in field plots of isogenic sorghum because the revertant is taller than its surrounding siblings. Seven *dw3* revertants were identified in rows of recombinant inbred lines of BTx623 (*dw3dw3*) × IS3620c (*Dw3Dw3*) planted in College Station, Texas, fields in 2014 (Figure S1). The revertants and three of their nonrevertant siblings were genotyped by PCR to amplify a region of *dw3*; genotypes that contained one or two copies of the 882-bp DNA correspond to the functional and nonfunctional alleles, respectively. The primers used were designed by Farfan *et al.* (2012).

Calculation of the light extinction coefficient k

Light interception throughout crop canopies is often formalized as an extinction coefficient k (as derived in Beer-Lambert's law) that relates the attenuation of light with properties of the material through which the light travels (Monteith and Moss 1977; Monsi and Saeki 2005; Nobel 2005; Long *et al.* 2006). Here we use the equation

$$I(x) = I_0 e^{-kx} \tag{1}$$

Given data $\{x_n, I(x_n)\}_{n=1}^N$, where $I(x)$ is the intensity (power per unit area) of radiation from the sunlight at depth x down the canopy, we can estimate the light extinction coefficient k by fitting with the Levenberg-Marquardt algorithm for nonlinear least squares (Jones *et al.* 2001). A detailed explanation of the function and its adoption to describe the vertical distribution of sunlight in a crop canopy is provided in File S1. We use k as a descriptor to characterize and compare the distribution of light in simulated and field-grown sorghum canopies with differing leaf inclination angles.

Virtual sorghum canopies

We constructed functional-structural plant models of sorghum and collected depth and incident-light data $\{x_n, I(x_n)\}_{n=1}^N$ in

simulated light environments and calculated values of theoretical k. The three-dimensional virtual sorghum plants were constructed using Lindenmeyer systems in L-py (Boudon *et al.* 2012). Lindenmeyer systems provide a set of production rules whereby plant structural models are produced by recursion through phytomers (Prusinkiewicz *et al.* 2012). The virtual canopies were then illuminated by the nested radiosity model as implemented in CARIBU (Chelle and Andrieu 1998; Chelle *et al.* 2004; Pradal *et al.* 2008) given light input that reflected solar conditions in College Station, Texas (data retrieved from the U.S. Naval Observatory, aa.usno.navy.mil). Details on methods of construction and the scripts used can be found in File S2.

Field experimental sorghum canopies

Two sorghum RILs, RIL 63 and RIL 73, were identified as lines with large phenotypic variation in leaf angle when phenotyping the R07018 × R07020 RIL population grown under greenhouse conditions (Bartek *et al.* 2012). To study the effect of leaf angle on light penetration at different depths in the plant canopy, two adjacent plots, one plot of RIL 63 and one plot of RIL 73, were planted in College Station, Texas, fields (W96°20", N30°37"); each plot had four rows with row spacing of 0.76 m^2 and was planted at a density of 13.2 plants/m^2. To estimate k values for each of the two plots, light penetration at multiple layers in the canopy was measured for seven collections using two lifts and two PAR meters (LP-80, Decagon Devices, Inc., Pullman, Washington) to simultaneously take readings at the same canopy height in the two canopies (File S1, Figure S2, and Table S1). All plot and plant measurements along with raw depth from the experimental field data, subsequent scaling employed, and their fits to equation (1) are available in File S2.

Estimating potential biomass gain

The calculation of biomass yield gain is based on the gain of solar conversion efficiency on a per-leaf basis of C4 plants. We used energy absorbed at each sequential leaf through the canopy (predicted by the CARIBU model) and estimated the conversion efficiency provided by Zhu *et al.* (2010). Conversion efficiency is modeled as a linear parameter in the Monteith equation for biomass (Zhu *et al.* 2010), and thus the biomass yield gain is the same amount as the efficiency gain. The calculations made are available in File S2 as a spreadsheet.

Data availability

Data and analyses, including genetic maps, genotypes, phenotypes, and analysis code are contained in File S2, hosted at https://github.com/mulletlab/leafangle_supplement.

Results

Genetic regulation of sorghum leaf angle

Given that leaf inclination angle is associated with productivity increases in other crop plants (Sinclair and Sheehy 1999; Duvick 2005; Tian *et al.* 2011; Mansfield and Mumm 2014), we sought to identify genetic loci that regulate leaf angle in sorghum. Identification of genetic loci that modulate leaf angle will enable both experimental analyses of the effect of leaf angle on radiation use efficiency (RUE) and nitrogen status and deployment of favorable alleles into breeding programs. Genetic analyses were carried out using two RIL populations derived from the following biparental crosses: (1) grain sorghum lines BTx623 and IS3620c and (2) late-flowering bioenergy sorghum lines R07018 and R07020.

Leaf angle is developmentally regulated and changes based on leaf age; leaves at the top of a plant typically have small leaf angles and minimal variation that could be attributed to genetics (see File S1). As such, the angles of the third and fourth (and fifth when not senesced) fully expanded ligulated leaves, counting from the uppermost fully expanded leaf at the top of the plant, were measured in the two RIL populations at varying stages of development as grown in the field and in greenhouses (Table 1). Model selection of multiple-QTL mapping analyses as described in Manichaikul *et al.* (2009) identified three loci in the grain population (BTx623 × IS3620c) and four loci in the bioenergy population (R07018 × R07020) that affected leaf inclination angle ($P < 0.001$; Table 2). In a given population, leaf number, and environment, the proportion of phenotypic variance explained by the multiple-QTL model was always greater than 15%. Given that the small population sizes used here for mapping can inflate QTL variance estimates via the Beavis effect (Beavis 1994, 1998; Xu 2003), we also estimated the proportion of phenotypic variance explained by genome-wide SNPs and indels, as described in Yang *et al.* (2011). Given the relatedness of individuals in the populations, the proportion of phenotypic variance explained by the SNPs and indels using a GRM and REML (as implemented in GCTA) approximates the narrow-sense heritability of the trait (Yang *et al.* 2013). Heritabilities of each leaf angle ranged from 9 to 62% depending on the population, location, and plant age (Table 2). Heritabilities in the BTx623 × IS3620c population were much larger owing to the large effect of the *dw3* locus (discussed later); the dominant *Dw3* allele is fixed in R07018 and R07020 and does not segregate in the bioenergy population (Figure S3).

dwarf-3 regulates leaf angle in sorghum

Comparisons between QTL mapping results for leaf inclination angle and plant height in the BTx623 × IS3620c RIL population showed identical marker association with both traits across an interval of chromosome 7 corresponding to the *dwarf-3* (*dw3*) locus (data not shown). Previous reports also correlated alleles of *dw3* with stem dwarfing and leaf inclination angle (Hart *et al.* 2001). Furthermore, *dw3* is known to segregate in this mapping population, where BTx623 (*dw3dw3*) carries the nonfunctional *dw3*, an unstable allele that contains an 882-bp direct duplication that can revert to *Dw3* by unequal crossing over (Multani *et al.* 2003), and IS3620c (*Dw3Dw3*) contains the functional *Dw3* allele.

Table 2 Trait heritability and QTL of leaf inclination angle

Cross	Phenotyped	Leaf no.	Heritability ($\widehat{h^2}$)	QTL		
				Chr.	LOD$_2$ (Mbp)	Variance (%)
BTx623 × IS3620c	Fields; 90 DAP (n = 88)	3	0.62***	7	57.6–59.1[a]	37
		4	0.60***	1	55.6–60.4	12
				7	57.6–59.2[a]	38
	Greenhouse; 38 DAP (n = 336)	3	0.54***	7	58.3–58.8[a]	37
		4	0.50***	5	2.7–4.8	5
				7	58.3–58.8[a]	33
R07018 × R07020	Greenhouse; 39 DAP (n = 94)	3	0.39***	1	53.7–54.8[b]	24
		4	0.31***	1	13.6–61.3[b]	20
	Fields; 80 DAP (n = 94)	3	0.12**	7	55.2–58.3[b]	16
		4	0.23**	1	13.1–54.7[b]	19
		5	0.33***	1	13.1–15.2[b]	20
				1	53.4–54.7[b]	17
	Fields; 114 DAP (n = 94)	3	0.09*	3	5.6–61.1[b]	16
		4	0.12**	3	51.4–60.1	16
		5	0.14**	3	56.5–59.5	22

Estimates of trait heritability $\widehat{h^2}$ were approximated from estimations of variance explained by SNPs and indels across the genome for each phenotype (Yang *et al.* 2013). ***, **, and * denote *P*-values less than 0.0001, 0.05, and 0.1, respectively, for testing the null hypothesis that the trait is not heritable. All QTL models were chosen via model selection of multiple-QTL mapping analyses, as described in Manichaikul *et al.* (2009). All QTL were additive and have *P*-values < 0.001. The biparental cross, phenotype location (field or greenhouse), number of days after planting (DAP), individuals (*n*), and leaf number assayed in each experiment are given as metadata. The physical position [Sbi1, Paterson *et al.* (2009)] of largest LOD for each QTL and other statistics on the QTL models can be found in File S2.
[a] LOD$_2$ intervals that contain the *dw3* gene (chromosome *7*: 58.55–58.56 Mbp).
[b] LOD$_2$ intervals in which RILs 63 and 73 (the RILs used in field measurements of light extinction) are not genotypically identical.

The large phenotypic effect of the dominant *Dw3* allele on height enables identification of tall revertants among *dw3dw3* RILs. Therefore, we screened a field-grown subset of the BTx623 × IS3620c RIL population and identified revertant plants in seven different RIL plots by their increased heights. We found that the revertant plants with increased height also displayed large leaf inclination angles relative to nonrevertant plants (Figure 1 and Figure S1). Genotypes at the *dw3* gene confirmed that the dominant *Dw3* allele was present in the tall revertant plants. *Dw3* revertant plants showed increases in leaf inclination angle of up to 34° (0.59 rad) relative to *dw3* plants that were otherwise genetically identical individuals (Figure S1). Thus sorghum *dw3* has a pleiotropic effect on both height and leaf angle.

Leaf angle affects vertical light distribution in sorghum canopies

Once genetic loci regulating leaf inclination angle were identified, we sought to determine whether leaf inclination angle affects the distribution of solar radiation in the sorghum canopy and confers a functional difference in performance. To characterize and compare light interception by sorghum canopies with different leaf angles, the light extinction coefficients *k* of sorghum canopies were determined by modeling and using data from field measurements [equation (1)]. Given the same amount of available PAR, decreases in *k* translate to less PAR intercepted by upper layers of the canopy and more PAR available for interception at lower levels of the canopy (*i.e.*, closer to the ground) (Monsi and Saeki 2005). We first compared the light extinction coefficient *k* of two simulated vegetative-phase grain sorghum canopies that intercepted all available light (Chelle *et al.* 2004; Pradal *et al.* 2008; Boudon *et al.* 2012).

Plants in the simulated plots varying only in the leaf inclination angles of their fully expanded leaves were modeled under solar radiation conditions approximating a cloudless day in College Station, Texas, on July 13, 2013 (retrieved from U.S. Naval Observatory, aa.usno.navy.mil) (Figure 2A). The canopies with larger leaf inclination angles had a *k* that was two times larger than canopies with smaller leaf inclination angles, indicating that light was distributed more uniformly and deeper into the canopies of plants with small leaf inclination angles (Figure 2B).

To determine the extent that leaf inclination angle alters light distribution in canopies under field conditions, we identified two RILs from a biparental cross of bioenergy sorghum lines (R07018 × R07020), RIL 63 and RIL 73, that were phenotypically similar in all leaf traits measured except for leaf inclination angle (Figure S4). RIL 63 had a smaller leaf inclination angle at all phytomers compared to RIL 73 (Figure S4). Notably, RILs 63 and 73 from the R07018 × R07020 population had genotypic differences in three of the four QTL intervals affecting leaf angle identified by multiple-QTL mapping (indicated by *b* in Table 2); these genetic differences may underlie the large phenotypic differences in leaf inclination angle observed in these RILs. The two RILs were phenotypically similar with respect to stand density, leaf morphology, phytomer stem diameter and spacing, and biomass per unit height (Figure S4). Notably, RILs 63 and 73 varied with respect to the number of phytomers, leading to a difference in height and total biomass. Because of this height difference, measurements of *k* were scaled to percentage of canopy depth rather than absolute depth, although relative ordering of *k* values remains the same whether depth is
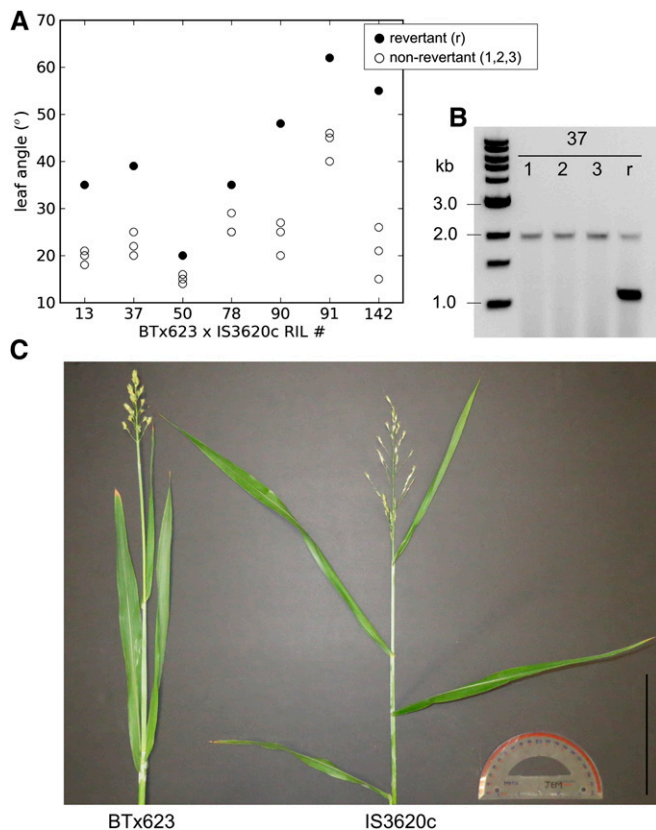
Figure 1 *dw3* regulates leaf inclination angle. (A) Leaf 3 inclination angles of revertants (r) in filled black circles and nonrevertants (1, 2, 3) in empty white circles of seven RILs of BTx623 × IS3620c. (B) Genotypes of revertants and nonrevertants of RIL 37 at the *dw3* locus using primers that flank the 882-bp tandem repeat that makes *dw3* nonfunctional; unequal crossing over can lead to excision of one repeat copy and spontaneous reversion to the functional *Dw3* allele (Multani *et al.* 2003; Farfan *et al.* 2012) (see Figure S1 for other RIL genotypes). (C) Parents, BTx623 and IS3620c, of the experimental cross in which revertants of *dw3* were identified grown under greenhouse conditions. The protractor used to measure all leaf inclination angles here is also shown, and the scale bar is 6 inches.

scaled or not (Table S1). Four row plots of RILs 63 and 73 were planted in the field at College Station, Texas, in 2014 and analyzed after canopy closure in July. PAR was measured throughout the canopy seven times over the course of 4 days using two PAR meters mounted on a platform that could be moved to varying heights in the canopies (Figure S2 and Table S1). Six of the data sets showed that the plots containing plants with smaller leaf inclination angles distributed PAR to greater depths in the canopy, with two of the seven showing that the k of the large leaf inclination angle plots is more than twice as large as the k of the small leaf inclination angle plot (Figure 2D and Table S1).

While RILs 63 and 73 were phenotypically similar for most measured traits and genotypically different at most detectable leaf angle QTL (Table 2 and Figure S4), the possibility remained that their differences in light canopy penetration arose from factors not captured by the experiment, such as additional QTL regulating plant architecture. To investigate

this possibility, simulated plants were parameterized using the measured phenotypes of RILs 63 and 73, including differences in phytomer number (and, consequently, height); traits not measured, such as leaf curvature, were kept constant, and the simulated plants were illuminated using field conditions. The light distribution plots generated by simulations were qualitatively similar to the field results (Figure 2, E and D). The possibility that differences in plant height and not leaf inclination angle were responsible for the smaller k of the small-angle plant was ruled out by removing phytomers so that the plant with small leaf angles, simulated RIL 63, was the same height as the plant with large leaf angles, simulated RIL 73; large leaf angles still caused k to be larger than small leaf angles (Figure S5). Fitting of the light extinction function [equation (1)] to the data revealed that the extinction model may not fully capture changes that occur in lower portions of the canopy (Figure 2, D and E). This suggests that the light extinction model's assumption of a homogeneous canopy is an oversimplification (Song *et al.* 2013) and that factors such as leaf orientation and leaf senescence may need to be considered in future adjustments to the model.

We next determined whether the redistribution of incident PAR would be predicted to have a functional impact on biomass accumulation. Using estimates of conversion efficiency obtained from Zhu *et al.* (2010), we found that the redistribution of incident PAR in the simulated canopy with small leaf angles would cause an increase in overall conversion efficiency relative to the large leaf angle canopy. From this, we extrapolated a conservative estimate of biomass accumulation during a bioenergy sorghum growing season without water or nutrient limitations. For the virtual sorghum and lighting in Figure 2A, the conversion efficiency of the canopy with smaller leaf angles is predicted to be 1.0436 of the conversion efficiency of the canopy with large leaf angles. If we further assume that (1) the 4% gain in conversion efficiency is realized for 4 hr (midday) per 14-hr day and (2) the effect calculated is applicable to the duration of vegetative closed-canopy growth, then given a bioenergy sorghum growing season where 140 days are in the vegetative closed canopy of its 200-day growing season (Olson *et al.* 2012), we predict an overall increase of 3% conversion efficiency over the entire growing season. Thus, under these conditions, the canopy with smaller leaf angles has the potential to accumulate 3% more biomass than the canopy with large leaf angles. Since these performance differences are predicted from morphologically reasonable canopy parameters, leaf angle represents a realistic target to improve biomass yields without increasing input.

Discussion

This study has shown that leaf inclination angles are genetically regulated in *S. bicolor* and that leaf angle alters the vertical distribution of solar radiation in closed canopies under field conditions. The improved distribution of solar radiation is predicted to improve photosynthetic conversion
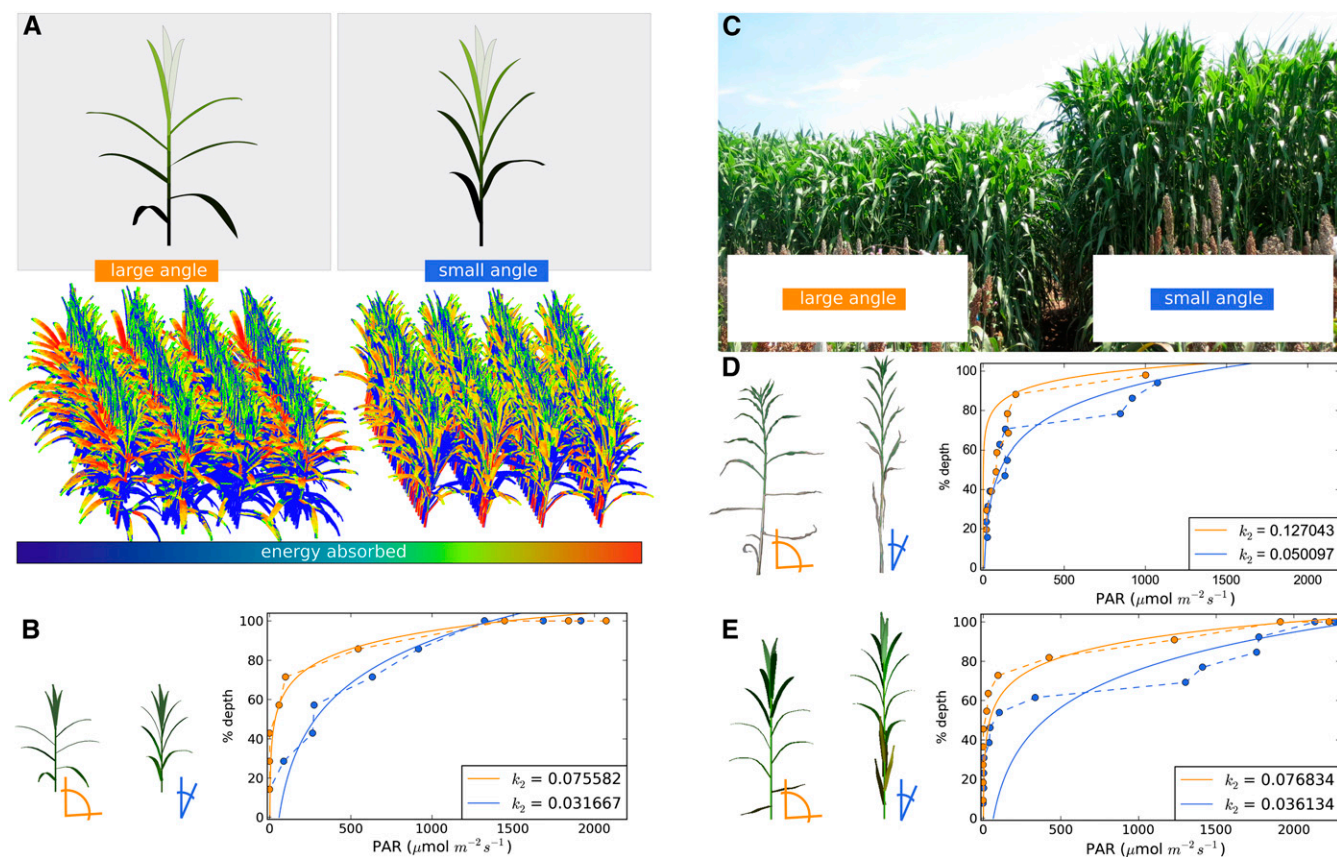
Figure 2 Leaf inclination angle affects light distribution in sorghum canopies. (A) Virtual sorghum plants and sorghum plots that vary in their leaf inclination angles (orange represents a larger leaf inclination angle relative to blue). (B) Light extinction curves for virtual plots from panel A simulated under solar conditions representing 13:00 on July 13, 2013, in College Station, Texas (W96°20", N30°37"). (C) Field plots of RIL 63 and RIL 73 from which light measurements were taken. (D) Light extinction curves for field plots from panel C assayed around 15:30 on July 22, 2014, in College Station, Texas. (E) Light extinction curves for virtual plots representing RIL 63 and RIL 73 simulated under solar conditions representing 15:30 on July 22, 2014, in College Station, Texas. In both simulation and field studies, plots with smaller leaf inclination angles fit a smaller light extinction coefficient k_2 relative to plots with larger leaf inclination angles (panels B, D, and E). k_2 values are derived from fits to equation (2) (see *Materials and Methods*).

efficiency of the canopy, resulting in a 3% gain in biomass yield for bioenergy sorghum. We found that the phenotypic difference in leaf angle between RIL 63 and RIL 73 corresponded with genotypic differences at most leaf angle QTL identified in the population from which they originated and that RIL 63 (with smaller leaf inclination angles) had a smaller light extinction coefficient k than RIL 73. Interestingly, RIL 63 also had more green leaf area and greater biomass than RIL 73. Additionally, while RIL 63 was taller, the length of each phytomer and biomass per unit height were similar (Figure S4), indicating that RIL 63 had an increased rate of phytomer production. This increase in phytomers and, in turn, biomass is consistent with the possibility that the small leaf angles of RIL 63 improved light interception and canopy conversion efficiency relative to RIL 73. Leaf appearance rate, or phyllochron, varies among sorghum genotypes during development and in response to the environment (Clerget *et al.* 2008; van Oosterom *et al.* 2011). In maize, field radiation intensity was negatively correlated with phyllochron (Birch *et al.* 1998). Determining whether the increased phyllochron in the small leaf angle genotype is

a consequence of (1) differential genetic regulation of phyllochron, (2) lower radiation interception by upper leaves, and/or (3) increased photosynthetic conversion efficiency of the canopy will be investigated in future experiments. Additionally, prior work in maize and rice predict that the small leaf angles of RIL 63 will enable higher biomass accumulation at higher planting densities relative to RIL 73, so the effects of planting density also should be investigated (Lambert and Johnson 1978; Sakamoto *et al.* 2006).

Identification of *dwarf-3*, which encodes a P-glycoprotein that modulates polar auxin transport, as a regulator of leaf inclination angle by up to 34° (0.59 rad) in sorghum was shown by analysis of naturally occurring revertants. As with height, the action of the null *dw3* allele on leaf angle is likely a consequence of reduced polar auxin transport from the shoot apical meristem (Multani *et al.* 2003; Knoller *et al.* 2010). Auxin was shown to regulate the establishment and propagation of the preligule band in maize plants with null alleles of *liguleless1*, *liguleless2*, and *liguleless narrow* (Moon *et al.* 2013), and P-glycoprotein (PGP) genes interact with PIN genes to influence local auxin distribution (Blakeslee

et al. 2007; Mravec et al. 2008). Furthermore, rice *LAZY1*, a polar auxin transport repressor, regulates rice tiller angle via shoot gravitropism (Li et al. 2007; Dong et al. 2013), and maize *ZmCLA4*, an ortholog of rice *LAZY1*, increases shoot gravitropism and leaf angle at elevated expression levels (Zhang et al. 2014). Additional work will be necessary to determine the mechanism by which *dw3* alleles regulate leaf angle. *dw3* also regulates sorghum height, and the pleiotropic effects of *dw3* explain observations from the sorghum literature, including a positive correlation between height and leaf angle in a sorghum grain association panel and increased leaf angle in some *dw3* NILs (George-Jaeggli et al. 2013; Perez et al. 2014).

While *dw3* had the largest effect on leaf angle of the loci reported here, the utility of *dw3* for modulating leaf angle to improve sorghum productivity may be limited by its pleiotropic effects on height. Previous work has shown that the reduction in shoot biomass caused by *dw3* reduces RUE and grain yield, which would likely offset any benefit afforded by small leaf angle for grain and bioenergy applications (George-Jaeggli et al. 2011, 2013). If the reduced productivity of grain sorghum with recessive *dw3* is due to a reduction in stem reserves, as proposed by George-Jaeggli et al. (2011), any conversion efficiency benefits conferred by leaf angle would be constrained by the sink limitation caused by reduced stem size. The efficiency benefits of small leaf angles caused by the null *dw3* allele may not be observed until recessive *dw3* is put into a genetic background that is not sink limited. For bioenergy applications, it is likely that the reduction in height and biomass caused by recessive *dw3* outweighs any productivity gains afforded by leaf angle, and other means of reducing leaf angle will be necessary. Fortunately, the genetic architecture underlying RIL 63 is promising because small leaf angles were associated with increased height and biomass.

In nature, large leaf angles may have been under positive selection because shading nearby plants would reduce competitors' ability to compete for light and nutrients (Schmitt et al. 2003; Drewry et al. 2014). In monoculture grain cropping systems, small leaf angle has been under positive selection because this trait enables higher planting density and higher grain yield, presumably due to the benefits of improved RUE and increased nitrogen content of canopies (Drewry et al. 2014; Warnasooriya and Brutnell 2014). The design of C4 energy grass crops is at an early phase of development and could benefit from improved RUE afforded by small leaf angles (Mullet et al. 2014). Energy sorghum and grain sorghum canopies close 60–75 days after seedling emergence, approximately when grain sorghum reaches anthesis. In contrast, energy sorghum remains vegetative following canopy closure for an additional 140 days, and plants retain a whorl of developing leaves at the top of the canopy that have very small angles (Olson et al. 2012). In grain sorghum, from anthesis through grain maturity, canopies lack the whorl of leaves with small angles. As such, we expect that the potential effects of leaf angles on yield will vary depending on the duration of developmental phases of the crop.

This study identified significant genetic variation for leaf angle in sorghum germplasm that can be deployed in energy, forage, and grain sorghum breeding programs. The simulation and field results support the conclusion that smaller leaf inclination angles cause a redistribution of solar radiation in closed canopies resulting in greater photosynthetic conversion efficiency and greater biomass yield potential. Large-scale studies of energy sorghum hybrids differing in leaf angles will be required to determine the extent to which this trait can increase biomass yield under field conditions.

Literature Cited

Bartek, M. S., S. C. Murray, P. E. Klein, J. E. Mullet, and W. L. Rooney, 2012 QTL for biomass yield and composition in energy sorghum (*Sorghum bicolor* L. Moench). Proceedings of the Sun Grant National Conference: Science for Biomass Feedstock Production and Utilization, New Orleans. Available at: http://sungrant.tennessee.edu/NatConference/.

Beavis, W., 1994 The power and deceit of QTL experiments: Lessons from comparative QTL studies, pp. 250–266 in *Proceedings of the Forty-Ninth Annual Corn and Sorghum Industry Research Conference*. American Seed Trade Association, Washington, DC.

Beavis, W., 1998 QTL Analyses power, precision, and accuracy, pp. 145–162 in *Molecular Dissection of Complex Traits*, edited by A. Patterson. CRC Press, Boca Raton, FL.

Birch, C. J., J. Vos, J. Kiniry, H. J. Bos, and A. Elings, 1998 Phyllochron responds to acclimation to temperature and irradiance in maize. Field Crops Res. 59: 187–200.

Blakeslee, J. J., A. Bandyopadhyay, O. R. Lee, J. Mravec, B. Titapiwatanakun et al., 2007 Interactions among PIN-FORMED and P-glycoprotein auxin transporters in *Arabidopsis*. Plant Cell 19: 131–147.

Boudon, F., C. Pradal, T. Cokelaer, P. Prusinkiewicz, and C. Godin, 2012 L-py: an L-system simulation framework for modeling plant architecture development based on a dynamic language. Front. Plant Sci. 3: 76.

Broman, K. W., H. Wu, S. Sen, and G. A. Churchill, 2003 R/qtl: QTL mapping in experimental crosses. Bioinformatics 19: 889–890.

Burow, G. B., R. R. Klein, C. D. Franks, P. E. Klein, K. F. Schertz et al., 2011 Registration of the BTx623/IS3620C recombinant inbred mapping population of sorghum. J. Plant Reg. 5: 141–145.

Chelle, M., and B. Andrieu, 1998 The nested radiosity model for the distribution of light within plant canopies. Ecol. Modell. 111: 75–91.

Chelle, M., J. Hanan, and H. Autret, 2004 Lighting virtual crops: the CARIBU solution for open L-systems, p. 194 in *Proceedings of*

the 4th International Workshop on Functional-Structural Plant Models, Montpellier France, edited by C. Godin *et al.* UMR AMAP, Montpellier, France.

Clerget, B., M. Dingkuhn, E. Goze, H. F. W. Rattunde, and B. Ney, 2008 Variability of phyllochron, plastochron and rate of increase in height in photoperiod-sensitive sorghum varieties. Ann. Bot. 101: 579–594.

DePristo, M. A., E. Banks, R. Poplin, K. V. Garimella, J. R. Maguire *et al.*, 2011 A framework for variation discovery and genotyping using next-generation DNA sequencing data. Nat. Genet. 43: 491–498.

Dong, Z., C. Jiang, X. Chen, T. Zhang, L. Ding *et al.*, 2013 Maize *LAZY1* mediates shoot gravitropism and inflorescence development through regulating auxin transport, auxin signaling, and light response. Plant Physiol. 163: 1306–1322.

Drewry, D. T., P. Kumar, and S. P. Long, 2014 Simultaneous improvement in productivity, water use, and albedo through crop structural modification. Glob. Change Biol. 20: 1955–1967.

Drouet, J. L., and R. Bonhomme, 1999 Do variations in local leaf irradiance explain changes to leaf nitrogen within row maize canopies? Ann. Bot. 84: 61–69.

Duvick, D. N., 2005 Genetic progress in yield of United States maize (*Zea mays* L.). Maydica 50: 193–202.

Farfan, I. D. B., B. R. Bergsma, G. Johal, and M. R. Tuinstra, 2012 A stable *dw3* allele in sorghum and a molecular marker to facilitate selection. Crop Sci. 52: 2063–2069.

Foley, J. A., N. Ramankutty, K. A. Brauman, E. S. Cassidy, J. S. Gerber *et al.*, 2011 Solutions for a cultivated planet. Nature 478: 337–342.

George-Jaeggli, B., D. R. Jordan, E. J. van Oosterom, I. J. Broad, and G. L. Hammer, 2013 Sorghum dwarfing genes can affect radiation capture and radiation use efficiency. Field Crops Res. 149: 283–290.

George-Jaeggli, B., D. R. Jordan, E. J. van Oosterom, and G. L. Hammer, 2011 Decrease in sorghum grain yield due to the *dw3* dwarfing gene is caused by reduction in shoot biomass. Field Crops Res. 124: 231–239.

Gill, J. R., P. S. Burks, S. A. Staggenborg, G. N. Odvody, R. W. Heiniger *et al.*, 2014 Yield results and stability analysis from the sorghum regional biomass feedstock trial. BioEnergy Res. 7: 1026–1034.

Hammer, G. L., Z. S. Dong, G. McLean, A. Doherty, C. Messina *et al.*, 2009 Can changes in canopy and/or root system architecture explain historical maize yield trends in the US corn belt? Crop Sci. 49: 299–312.

Hart, G. E., K. F. Schertz, Y. Peng, and N. H. Syed, 2001 Genetic mapping of *Sorghum bicolor* (L.) Moench QTLs that control variation in tillering and other morphological characters. Theor. Appl. Genet. 103: 1232–1242.

Hurng, W. P., L. Y. Su, and C. H. Kao, 1986 Senescence of rice leaves: regulation by light. Bot. Bull. Academia Sinica 27: 163–174.

Jones, E., Oliphant, T., Peterson, P. *et al.*, 2001 SciPy: open source scientific tools for Python. Available at: http://www.scipy.org/. Accessed: July 10, 2014.

Knoller, A. S., J. J. Blakeslee, E. L. Richards, W. A. Peer, and A. S. Murphy, 2010 *Brachytic2/ZmABCB1* functions in IAA export from intercalary meristems. J. Exp. Bot. 61: 3689–3696.

Lambert, R. J., and R. R. Johnson, 1978 Leaf angle, tassel morphology, and performance of maize hybrids. Crop Sci. 18: 499–502.

Lee, E. A., and M. Tollenaar, 2007 Physiological basis of successful breeding strategies for maize grain yield. Crop Sci. 47: S202–S215.

Li, C. H., Y. X. Li, Y. S. Shi, Y. C. Song, D. F. Zhang *et al.*, 2015 Genetic control of the leaf angle and leaf orientation value as revealed by ultra-high density maps in three connected maize populations. PLoS One 10: e0121624.

Li, H., and R. Durbin, 2010 Fast and accurate long-read alignment with Burrows-Wheeler transform. Bioinformatics 26: 589–595.

Li, P., Y. Wang, Q. Qian, Z. Fu, M. Wang *et al.*, 2007 *LAZY1* controls rice shoot gravitropism through regulating polar auxin transport. Cell Res. 17: 402–410.

Long, S. P., X. G. Zhu, S. L. Naidu, and D. R. Ort, 2006 Can improvement in photosynthesis increase crop yields? Plant Cell Environ. 29: 315–330.

Manichaikul, A., J. Y. Moon, S. Sen, B. S. Yandell, and K. W. Broman, 2009 A model selection approach for the identification of quantitative trait loci in experimental crosses, allowing epistasis. Genetics 181: 1077–1086.

Mansfield, B. D., and R. H. Mumm, 2014 Survey of plant density tolerance in US maize germplasm. Crop Sci. 54: 157–173.

McCormick, R. F., S. K. Truong, and J. E. Mullet, 2015 RIG: recalibration and interrelation of genomic sequence data with the GATK. G3 5: 655–665.

McKenna, A., M. Hanna, E. Banks, A. Sivachenko, K. Cibulskis *et al.*, 2010 The Genome Analysis Toolkit: a MapReduce framework for analyzing next-generation DNA sequencing data. Genome Res. 20: 1297–1303.

McMullen, M. D., S. Kresovich, H. S. Villeda, P. Bradbury, H. H. Li *et al.*, 2009 Genetic properties of the maize nested association mapping population. Science 325: 737–740.

Monsi, M., and T. Saeki, 2005 On the factor light in plant communities and its importance for matter production. Ann. Bot. 95: 549–567.

Monteith, J. L., and C. J. Moss, 1977 Climate and the efficiency of crop production in Britain. Philos. Trans. R. Soc. Lond. Series B 281: 277–294.

Moon, J., H. Candela, and S. Hake, 2013 The Liguleless narrow mutation affects proximal-distal signaling and leaf growth. Development 140: 405–412.

Moreno, M. A., L. C. Harper, R. W. Krueger, S. L. Dellaporta, and M. Freeling, 1997 liguleless1 encodes a nuclear-localized protein required for induction of ligules and auricles during maize leaf organogenesis. Genes Dev. 11: 616–628.

Morishige, D. T., P. E. Klein, J. L. Hilley, S. M. E. Sahraeian, A. Sharma *et al.*, 2013 Digital genotyping of sorghum: a diverse plant species with a large repeat-rich genome. BMC Genomics 14: 448.

Mravec, J., M. Kubes, A. Bielach, V. Gaykova, J. Petrasek *et al.*, 2008 Interaction of PIN and PGP transport mechanisms in auxin distribution-dependent development. Development 135: 3345–3354.

Mullet, J., D. Morishige, R. McCormick, S. Truong, J. Hilley *et al.*, 2014 Energy sorghum: a genetic model for the design of C4 grass bioenergy crops. J. Exp. Bot. 65: 3479–3489.

Multani, D. S., S. P. Briggs, M. A. Chamberlin, J. J. Blakeslee, A. S. Murphy *et al.*, 2003 Loss of an MDR transporter in compact stalks of maize *br2* and sorghum *dw3* mutants. Science 302: 81–84.

Murchie, E., and M. Reynolds, 2012 Crop radiation capture and use efficiency, pp. 2615–2638 in *Encyclopedia of Sustainability Science and Technology*, edited by R. A. Meyers. Springer, New York.

Murchie, E. H., M. Pinto, and P. Horton, 2009 Agriculture and the new challenges for photosynthesis research. New Phytol. 181: 532–552.

Nobel, P. S., 2005 *Physicochemical and Environmental Plant Physiology*. Academic Press, New York.

Olson, S. N., K. Ritter, W. Rooney, A. Kemanian, B. A. McCarl *et al.*, 2012 High biomass yield energy sorghum: developing a genetic model for C4 grass bioenergy crops. Biofuels Bioprod. Bioref. 6: 640–655.

Paterson, A. H., J. E. Bowers, R. Bruggmann, I. Dubchak, J. Grimwood *et al.*, 2009 The *Sorghum bicolor* genome and the diversification of grasses. Nature 457: 551–556.

Pendleton, J. W., G. E. Smith, S. R. Winter, and T. J. Johnston, 1968 Field investigations of the relationships of leaf angle in corn (*Zea mays L.*) to grain yield and apparent photosynthesis. Agron. J. 60: 422–424.

Peng, B., R. K. Yu, K. L. Dehoff, and C. I. Amos, 2007 Normalizing a large number of quantitative traits using empirical normal quantile transformation. BMC Proc. 1(Suppl. 1): S156.

Perez, M. B. M., J. Zhao, Y. H. Yin, J. Y. Hu, and M. G. S. Fernandez, 2014 Association mapping of brassinosteroid candidate genes and plant architecture in a diverse panel of *Sorghum bicolor*. Theor. Appl. Genet. 127: 2645–2662.

Pradal, C., S. Dufour-Kowalski, F. Boudon, C. Fournier, and C. Godin, 2008 OpenAlea: a visual programming and component-based software platform for plant modelling. Funct. Plant Biol. 35: 751–760.

Prusinkiewicz, P., M. Shirmohammadi, and F. Samavati, 2012 L-Systems in geometric modeling. Int. J. Found. Comput. Sci. 23: 133–146.

Purcell, S., B. Neale, K. Todd-Brown, L. Thomas, M. A. R. Ferreira *et al.*, 2007 PLINK: a tool set for whole-genome association and population-based linkage analyses. Am. J. Hum. Genet. 81: 559–575.

Rooney, W. L., J. Blumenthal, B. Bean, and J. E. Mullet, 2007 Designing sorghum as a dedicated bioenergy feedstock. Biofuels Bioprod. Bioref. 1: 147–157.

Sakamoto, T., Y. Morinaka, T. Ohnishi, H. Sunohara, S. Fujioka *et al.*, 2006 Erect leaves caused by brassinosteroid deficiency increase biomass production and grain yield in rice. Nat. Biotechnol. 24: 105–109.

Schmitt, J., J. R. Stinchcombe, M. S. Heschel, and H. Huber, 2003 The adaptive evolution of plasticity: phytochrome-mediated shade avoidance responses. Integr. Comp. Biol. 43: 459–469.

Sinclair, T. R., and J. E. Sheehy, 1999 Erect leaves and photosynthesis in rice. Science 283: 1456–1457.

Song, Q. F., G. L. Zhang, and X. G. Zhu, 2013 Optimal crop canopy architecture to maximise canopy photosynthetic CO_2 uptake under elevated CO_2: a theoretical study using a mechanistic model of canopy photosynthesis. Funct. Plant Biol. 40: 109–124.

Tian, F., P. J. Bradbury, P. J. Brown, H. Hung, Q. Sun *et al.*, 2011 Genome-wide association study of leaf architecture in the maize nested association mapping population. Nat. Genet. 43: 159–162.

Tollenaar, M., and J. Wu, 1999 Yield improvement in temperate maize is attributable to greater stress tolerance. Crop Sci. 39: 1597–1604.

Truong, S. K., R. F. McCormick, D. T. Morishige, and J. E. Mullet, 2014 Resolution of genetic map expansion caused by excess heterozygosity in plant recombinant inbred populations. G3 4: 1963–1969.

Van der Auwera, G. A., M. O. Carneiro, C. Hartl, R. Poplin, G. Del Angel *et al.*, 2013 From FastQ data to high confidence variant calls: the Genome Analysis Toolkit best practices pipeline. Curr. Protoc. Bioinformatics 11: 11.10.11–11.10.33.

van Oosterom, E. J., A. K. Borrell, K. S. Deifel, and G. L. Hammer, 2011 Does increased leaf appearance rate enhance adaptation to postanthesis drought stress in sorghum? Crop Sci. 51: 2728–2740.

van Zanten, M., T. L. Pons, J. A. M. Janssen, L. A. C. J. Voesenek, and A. J. M. Peeters, 2010 On the relevance and control of leaf angle. Crit. Rev. Plant Sci. 29: 300–316.

Walsh, J., C. A. Waters, and M. Freeling, 1998 The maize gene liguleless2 encodes a basic leucine zipper protein involved in the establishment of the leaf blade-sheath boundary. Genes Dev. 12: 208

Warnasooriya, S. N., and T. P. Brutnell, 2014 Enhancing the productivity of grasses under high-density planting by engineering light responses: from model systems to feedstocks. J. Exp. Bot. 65: 2825–2834.

Xin, Z., D. Gitz, G. Burow, C. Hayes, and J. J. Burke, 2015 Registration of two allelic erect leaf mutants of sorghum. J. Plant Reg. 9: 254–257.

Xu, S. Z., 2003 Theoretical basis of the Beavis effect. Genetics 165: 2259–2268.

Yang, J. A., S. H. Lee, M. E. Goddard, and P. M. Visscher, 2011 GCTA: a tool for genome-wide complex trait analysis. Am. J. Hum. Genet. 88: 76–82.

Yang, J. A., S. H. Lee, M. E. Goddard, and P. M. Visscher, 2013 Genome-wide complex trait analysis (GCTA): methods, data analyses, and interpretations, pp. 215–236 in Genome-Wide Association Studies and Genomic Prediction (Methods in Molecular Biology Series, Vol. 1019), edited by C. Gondo, J. van der Werf, and B. Hayes. Humana Press, New York.

Yoshida, S., 1972 Physiological aspects of grain yield. Annu. Rev. Plant Physiol. 23: 437–445.

Zhang, J., L. X. Ku, Z. P. Han, S. L. Guo, H. J. Liu *et al.*, 2014 The *ZmCLA4* gene in the *qLA4–1* QTL controls leaf angle in maize (*Zea mays* L.). J. Exp. Bot. 65: 5063–5076.

Zhao, S. Q., J. A. Hu, L. B. Guo, Q. A. Qian, and H. W. Xue, 2010 Rice leaf inclination2, a VIN3-like protein, regulates leaf angle through modulating cell division of the collar. Cell Res. 20: 935–947.

Zhu, X. G., S. P. Long, and D. R. Ort, 2008 What is the maximum efficiency with which photosynthesis can convert solar energy into biomass? Curr. Opin. Biotechnol. 19: 153–159.

Zhu, X. G., S. P. Long, and D. R. Ort, 2010 Improving photosynthetic efficiency for greater yield. Annu. Rev. Plant Biol. 61: 235–261.

Communicating editor: J. B. Holland

GENETICS

Harnessing Genetic Variation in Leaf Angle to Increase Productivity of *Sorghum bicolor*

Sandra K. Truong, Ryan F. McCormick, William L. Rooney, and John E. Mullet

Supplemental Information: Harnessing genetic variation in leaf angle to increase productivity of

Sorghum bicolor

Sandra K. Truong [1,2], Ryan F. McCormick [1,2], William L. Rooney [3], and John E. Mullet [1,2,*]

1 Interdisciplinary Program in Genetics, Texas A&M University, College Station, Texas 77843
2 Biochemistry & Biophysics Department, Texas A&M University, College Station, Texas 77843
3 Soil & Crop Sciences Department, Texas A&M University, College Station, Texas 77843

* Corresponding Author: John E. Mullet
                             300 Olsen Boulevard
                             College Station, TX 77843-2128
                             (979) 845 0722
                             jmullet@tamu.edu

File S1

Extended Materials and Methods

Calculation of the light extinction coefficient, k.

Light interception throughout crop canopies is often formalized as an extinction coefficient, k (as derived in Beer-Lambert's Law), that relates the attenuation of light with properties of the material through which the light travels (Monteith 1977; Monsi and Saeki 2005; Nobel 2005; Long *et al.* 2006). Here, we describe adoption of Beer-Lambert equations in the context of solar radiation attenuation through a sorghum canopy to characterize and compare the distribution of light in simulated and field grown sorghum canopies with differing leaf inclination angles.

Let $I(x)$ be the intensity, power per unit area, of radiation from the sunlight at depth x down the canopy. For any given time at a plane above the canopy, $x = 0$, the intensity of radiation from the sun is at its maximum as no radiation has been intercepted, $I(0) = \max_x I(x)$. A sequence of planes, parallel to the ground, moving from the top, $x = 0$, down to the ground level of the canopy will have decreasing amounts of transmitted radiation, as each plane in the canopy intercepts a portion of the radiation. As such, the rate of radiation or light extinction when moving down the canopy, $\frac{dI}{dx}$, can be represented as

$$\frac{dI}{dx} = -kI(x), \tag{1}$$

where k is a dimensionless variable that represents the proportion of radiation intercepted at depth x down the canopy. By integration of Equation 1 and the initial condition $I(0) = I_0$,

$$I(x) = I_0 e^{-kx} \tag{2}$$

Thus given data, $\{x_n, I(x_n)\}_{n=1}^{N}$, that can be reasonably described by Equation 2, we can find light extinction coefficient, k, and use this as a descriptor for the distribution of light down a sorghum canopy. We defined I_0, the top of canopy, to be the plane immediately below the whorls of plants in the canopy. We distinguish between two groups of leaves in a sorghum canopy: (i) the whorl, the top of the plant from which leaves emerge, (ii) and leaves that are fully expanded below the whorl. The whorl contains leaves that are essentially in the same plane, whereas fully expanded leaves share less planes with other leaves above and below it. We found better fits to light data when fitting data just below the whorl to find the light extinction coefficient, k_2, however the relative relationship between small and large leaf inclinations angles remained regardless of where we defined the top of the canopy. The next sections will describe the method used to collect the data in both simulated and field experiments to estimate light extinction coefficients, ks. Specifically, k values for simulated and experimental data were solved for by the Levenberg-Marquardt algorithm for non-linear least-squares as implemented in the open source software SciPy's scipy.optimize.curve_fit() function (Jones 2001).

Virtual sorghum canopies.

In order to calculate theoretical ks we constructed functional-structural plant models of sorghum and collected depth and incident light data, $\{x_n, I(x_n)\}_{n=1}^{N}$, in simulated light environments. The 3-dimensional virtual sorghum plants were constructed using Lindenmeyer systems in L-py (Boudon *et al.* 2012). Lindenmeyer-systems provide a set of production rules whereby plant structural models are produced by recursion through phytomers (Prusinkiewicz *et al.* 2012). As such, virtual sorghum was constructed from phytomers, characterized by a stem and a leaf that emerges on top of one other. Thus each sorghum plant has a set of phytomers $p = p_1, p_2, \ldots, p_N$ where p_1 is the first phytomer to emerge and closest to the bottom and p_N is the last fully emerged phytomer at the top of the plant; only the colored phytomers are considered to calculate k_2 (Figure 2a). These virtual plants were then replicated to simulate sorghum plots that have typical row spacing of 0.76 m and planting density of 13.2 plants/m^2. Since the phytomers appear one on top of another and are uniformly distanced from the ground in the virtual environment, fully emerged phytomers, p_i, are used as depth measurements in the virtual sorghum canopies. When the simulated sorghum genotypes varied in the number of the phytomers (and consequently height) as they did when simulating plants with the characteristics of RIL 63 and RIL 73 of the R07018 x R07020 recombinant inbred line population, the height difference was accounted for by scaling depth to be a percentage depth, such that $x_n := 100 \frac{p_n}{p_N}$. The qualitative relationship of the rates of extinction between canopies with large and small leaf angles remains the same whether or not scaling is performed; scaling height just removes an unnecessary complexity.

The virtual canopies were then illuminated by the nested radiosity model as implemented in CARIBU (Chelle and Andrieu 1998; Chelle 2004) given light input that reflected solar conditions in College Station, TX (data retrieved from The United States Naval Observatory). The illuminated sorghum canopies could then be visualized (see Supporting Information for a .gif time course of lighting over a day). The nested radiosity model enables the estimation of absorbed energy or irradiance of each phytomer. Construction and lighting of the virtual canopies were all done within the open source software OpenAlea v1.0 that integrates L-py and Caribu, among other functional-structural modeling tools (Pradal *et al.* 2008). Let $Eabs(p_n)$ be the energy absorbed by phytomer n, p_n. Then to extract the amount of energy or incident light available, $I(x_n)$, at x_n

$$I(x_n) = \sum_{i=1}^{N} Eabs(p_i) - \sum_{i=n}^{N} Eabs(p_i).$$

With Equation 2 and p_n defined, this provides data, $\{x_n, I(x_n)\}_{n=1}^{N}$, to fit to Equation 2 in order to estimate ks for virtual sorghum canopies. Input files and scripts to reproduce virtual sorghum canopies used here are accessible on GitHub (see Supplemental Information).

Field experimental sorghum canopies.

To collect incident light data at different depths in the sorghum canopies, two lifts for PAR meters were used to take simultaneous readings in two plots of sorghum. Each of the two plots contained four rows of the same genotype, where the two genotypes varied in their leaf inclination angle. Two sorghum recombinant inbred lines, RIL 63 and RIL 73, were identified as RILs that had varying inclination angles under genetic regulation when QTL mapping was performed in a RIL population generated from a biparental cross of the energy sorghum lines R07018 and R07020 (Bartek 2012). These two genotypes were then planted in 4 row plots with row spacing of 0.76 m^2 and planting density of 13.2 plants/m^2 in College Station, TX fields (W 96 20, N 30 37).

The consistent depths at which incident sunlight was captured in the canopies were ensured by using two pulley systems that were individually manned. Figure S3 shows the pulley and the PAR meters, LP-80 from Decagon Devices. The platforms holding the LP-80 were raised and lowered in increments of 1 ft ($0.3048\ m$) that were marked on the pulley string to guide the depth in canopy where n are the depth measurements that the PAR meter is n ft from ground, $n = 1, \ldots, 14$. The genotypes were different heights at the time of measurement, during their vegetative stage; percentages of depth with respect to height of genotype, $h_{genotype}$, in the canopies are used such that $x_n := 100\frac{n}{h_{genotype}}$. The rates of extinction for large and small leaf angle canopies remained the same whether or not depth was scaled, so depth was scaled to remove complexity. One set of readings represents the depths measured from top to bottom or bottom to top by the operators. To mitigate operational biases, the operators, PAR meters, and pulley systems were often swapped between plots. Lastly, consistency of external light conditions between the plots were maintained by using the two PAR meters and coordination between the operators so that the same depths were assayed simultaneously in both plots. Two of the sets of data, those taken on July 25th, were taken after the plots had been thinned to a lesser density; the change in plot density increased the amount of PAR available at lower levels in the canopy, but did not change the relative trend of light extinction (Table S2).

The platform and pulley mechanism was designed to reduce interference with the 0.865 m probe that contains 80 PAR sensors and was used in between the two middle rows of the 4 row plots. The instrument was set to log PAR data, $I(t)$, automatically at 1 minute intervals, and 3 minutes were spent at each level in the canopy and recorded to ensure that at least two data points were captured at each level in the canopy. It took users manning the instruments different amounts of time to move the platform to the next level, and so data for the 3 minutes at each level began when both platforms were at the prescribed depth and cloud cover was absent. Light interception in the two plots was simultaneously assayed to ensure that the amount of available sunlight, I_0, was similar. Light intercepted at a given depth was taken as the average of logged PAR measurements that were available in the 3 minute windows. Let the 3 minute interval at depth x_n be $(t_0, t_T)_n$, then $I(x_n) := average_{t \in (t_0, t_T)_n} I(t)$. All plot and plant measurements along with raw depth from the experimental field data and subsequent scaling employed and their fits to Equation 2 are available in the Supplemental Information.
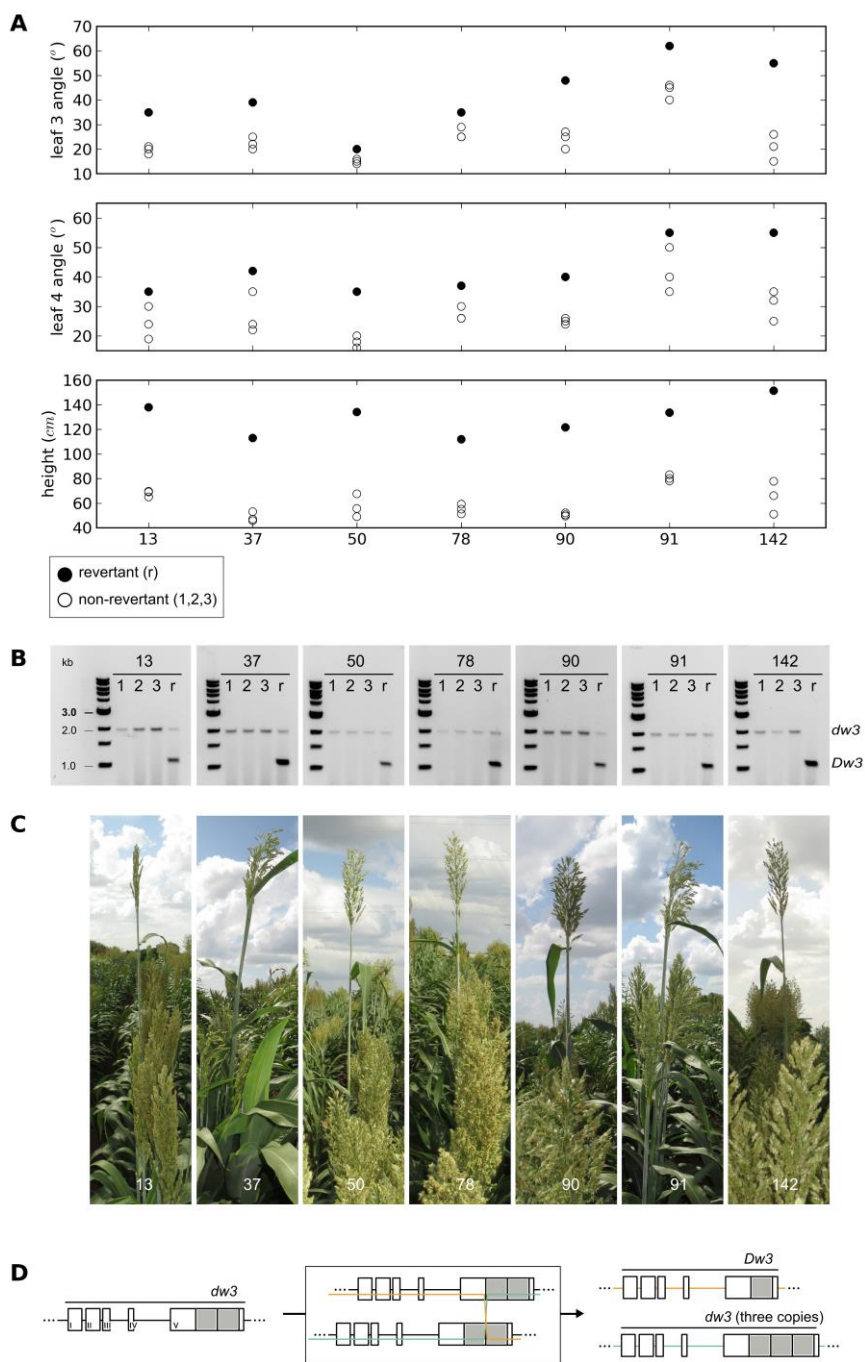
Figure S1 *dw3* **regulates leaf inclination angle. (A)** Phenotypes of *Dw3* revertants (r; filled circles) and non-revertants (1, 2, 3; open circles) of RILs of BTx623 x IS3620C **(B)** Genotypes of revertants and non-revertants of RILs at the *dw3* locus generated using primers designed by FARFAN *et al.* (2012) that flank the 882 bp tandem repeat that makes *dw3* non-functional. Unequal crossing over at *dw3* causes reversion. **(C)** Tall revertants in the row with short non-revertants were identified and genotyped **(A** and **B)** in the fields in College Station, TX. **(D)** This diagram shows the *dw3* non-functional allele with tandem repeats on exon V as two gray boxes. Unequal crossing over during meiosis results in a revertant functional *Dw3* and a non-functional *dw3* with three copies of the 882 bp sequence.

Figure S2 Lift for LP-80 PAR meter. (A) Image of the PAR meter lift used for collection of light measurements within canopies. **(B)** Images of the lift and PAR meter in preparation and in the sorghum canopy. There are views of the wooden platform that the LP-80 sits on and the PAR meter that takes measurements in the canopy. There is also an image of both lifts, where the one on the left has its metal poles extended to 10 ft and the one the right has poles extended to 15 ft.
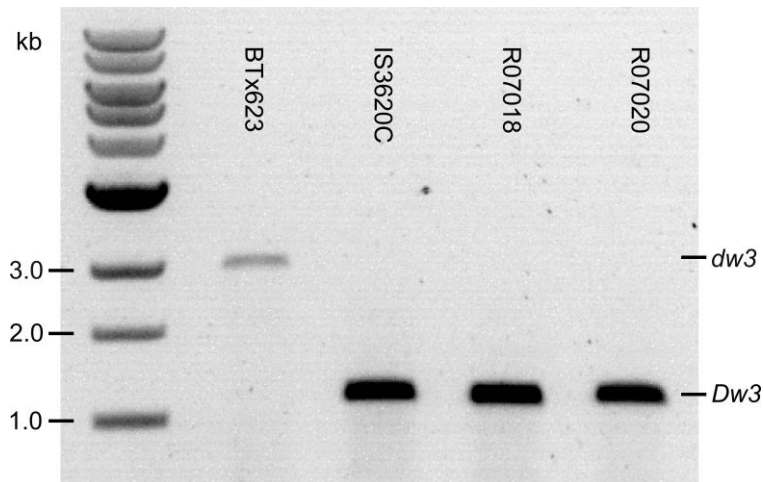
Figure S3 *dwarf-3* **genotypes of the bi-parental mapping populations.** BTx623, IS3620C, R07018, and R07020 were genotyped at the *dw3* locus generated using primers designed by FARFAN *et al.* (2012) that flank the 882 bp tandem repeat that makes *dw3* non-functional. BTx623 has non-functional *dw3* alleles, while IS3620C, R07018, and R07020 have functional *Dw3* alleles.
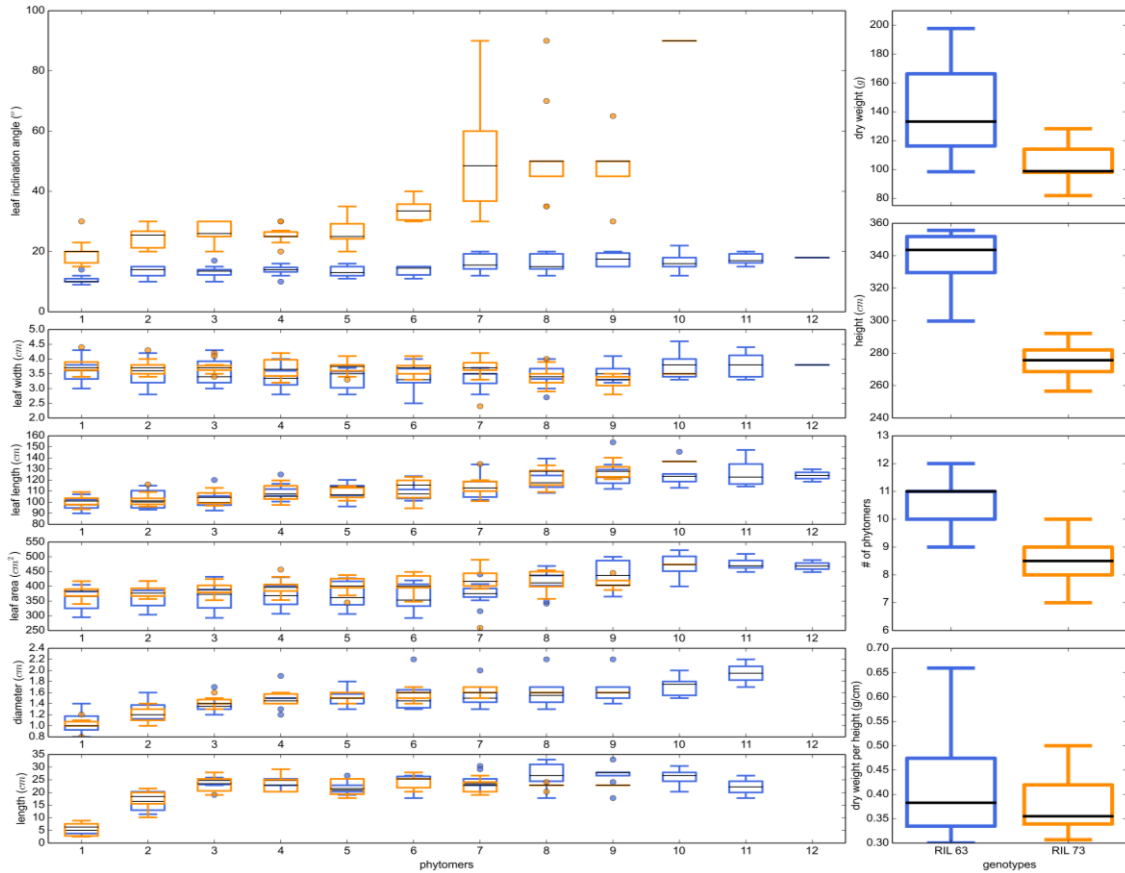
Figure S4   R07018 x R07020 RIL 63 & RIL 73 phenotypes. The boxplots show phenotype data from ten sorghum plants of RIL 63 (blue) and RIL 73 (orange) that were grown in 4-row plots in College Station, TX fields. On the left are measurements by phytomer, where phytomer 1 is at the top of the plant and corresponds to the phytomer with the most recent fully expanded leaf. On the right are measurements of the two genotypes. Leaf chlorophyll (SPAD) was also characterized: RIL 63 with $41.3 \pm 1.5 \; nmol/cm^2$ and RIL 73 with $44.7 \pm 4.0 \; nmol/cm^2$.
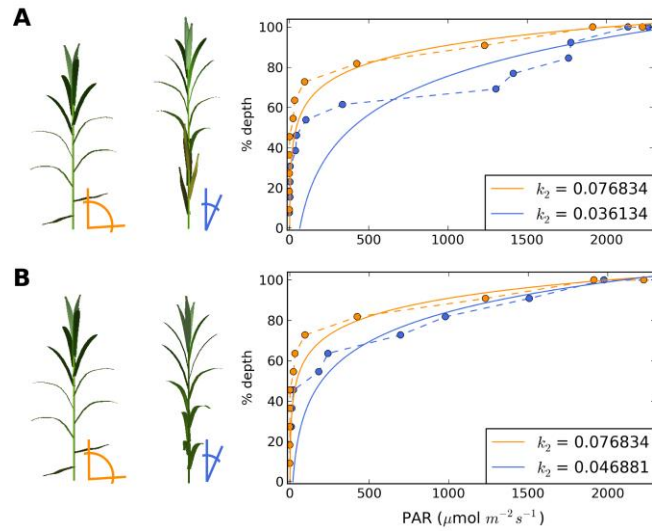
Figure S5 Leaf inclination angle regulates light distribution in canopies. (A) Images of RIL 63 and RIL 73 bioenergy sorghum plants (same as in Figure 2 of the main text). **(B)** Reducing the height of RIL 63 to be the same height as RIL 73 was done by decreasing the number of phytomers. The resulting k of RIL 63 remains smaller than RIL 73 in solar conditions representative of College Station, TX on July 22, 2014 at 15:30. While the qualitative relationship between k values of these plants remains unchanged with respect to height, the change in k that occurs when shortening a plant with RIL 63 angles indicates that height also plays a role in light distribution.

Table S1   Light distribution in canopies of RIL 63 and RIL 73.

	Height		Scaled depth	
Time of acquisition	RIL 73 (large)	RIL 63 (small)	RIL 73 (large)	RIL 63 (small)
July 22nd at 1400*	0.641993	0.426493	0.065483	0.054250
July 22nd at 1530*	1.245529	0.392925	0.127043	0.050097
July 23rd at 1440	0.576724	0.295480	0.060556	0.038412
July 24th at 1240	0.325723	0.332027	0.034201	0.043828
July 24th at 1350	0.389599	0.297924	0.040908	0.040220
July 25th at 1220*	0.374110	0.131663	0.038159	0.017116
July 25th at 1400*	0.395254	0.210151	0.040316	0.031041

k is calculated with and without scaling depth (height) and scaled depth; the qualitative relationship of ks between RIL 63 (small angles) and RIL 73 (large angles) remain the same. Data was retrieved in July 2014 on the given dates in College Station, TX. "*" denote datasets where RIL 63 was measured by LP-80 #2 and RIL 73 data was measured by LP-80 #1. The LP-80s were switched at other times.

File S2
Additional Supporting Folders and Files

Additional Supporting Folders and Files is available on https://github.com/mulletlab/leafangle_supplement/.

For a detailed work-through of virtual sorghum analysis, custom scripts, .lpy files, and associated parameters are in folder v_sorghum. Data pertaining to field experiments of RIL 63 and RIL 73, and analysis to find ks are in folder exp_fields. Specific parameters and additional information for the PCR amplification of *dw3* or *Dw3* are in folder dw3. Genotypes, phenotypes, correlation of phenotypes, genetic linkage maps, heritability calculations and statistics, and multiple QTL mapping penalized LOD scores for each phenotype and the statistics on QTL models presented are in folder h2_and_qtl.

References

Bartek, M. S., Murray, S.C., Klein, P.E., Mullet, J.E., & Rooney, W.L. , 2012 QTL for biomass yield and composition in energy sorghum (*Sorghum bicolor* L. Moench), pp. in *Science for Biomass Feedstock Production and Utilization SunGrant Conference*. SunGrant Initiative, New Orleans, Louisiana.

Boudon, F., C. Pradal, T. Cokelaer, P. Prusinkiewicz and C. Godin, 2012 L-py: an L-system simulation framework for modeling plant architecture development based on a dynamic language. Frontiers in Plant Science 3**:** 76.

Chelle, M., and B. Andrieu, 1998 The nested radiosity model for the distribution of light within plant canopies. Ecological Modelling 111**:** 75-91.

Chelle, M., Hanan J., & Autret, H. , 2004 Lighting virtual crops: the CARIBU solution for open L-systems, pp. 194 in *4th International Workshop on Functional-Structural Plant Models*, edited by C. Godin, Montpellier, France.

Farfan, I. D. B., B. R. Bergsma, G. Johal and M. R. Tuinstra, 2012 A stable *dw3* allele in sorghum and a molecular marker to facilitate selection. Crop Science 52**:** 2063-2069.

Jones, E., Oliphant, T., Peterson, P. et al., 2001 SciPy: Open source scientific tools for Python, pp.

Long, S. P., X. G. Zhu, S. L. Naidu and D. R. Ort, 2006 Can improvement in photosynthesis increase crop yields? Plant Cell and Environment 29**:** 315-330.

Monsi, M., and T. Saeki, 2005 On the factor light in plant communities and its importance for matter production. Annals of Botany 95**:** 549-567.

Monteith, J. L., & Moss, C.J., 1977 Climate and the efficiency of crop production in Britain Philosophical Transactions of the Royal Society of London, Series B: Biological Sciences 281**:** 277-294.

Nobel, P. S., 2005 *Physicochemical and environmental plant physiology*. Elsevier Academic Press, Amsterdam ; Boston.

Pradal, C., S. Dufour-Kowalski, F. Boudon, C. Fournier and C. Godin, 2008 OpenAlea: a visual programming and component-based software platform for plant modelling. Functional Plant Biology 35**:** 751-760.

Prusinkiewicz, P., M. Shirmohammadi and F. Samavati, 2012 L-Systems in geometric modeling. International Journal of Foundations of Computer Science 23**:** 133-146.